scientific data

Check for updates

OPEN

DATA DESCRIPTOR

A single-center 3D reconstruction image dataset for exploring inferior mesenteric artery and vein types

Zongxian Zhao, Xinyu Su, Shu Zhu, Yuan Yao & Zongju Hu ✉

The inferior mesenteric artery (IMA) and inferior mesenteric vein (IMV) are of critical significance in colorectal surgery; however, their anatomical variations and classification systems remain undefined. Additionally, existing studies lack open-source image datasets, which significantly hinder research reproducibility and academic collaboration in this field. In the dataset, we retrospectively collected 3D reconstructed images of IMA/IMV from 147 colorectal cancer patients, which were validated intraoperatively, and openly shared their variation types. As the first 3D image dataset focusing on IMA/IMV anatomical variations to date, this dataset serves as a valuable resource for research on IMA/IMV anatomical variations and an important reference for clinical training of colorectal surgeons.

Background & Summary

The large intestine is one of the major digestive tract organs and colorectal cancer (CRC) is one of the most prevalent malignancies of the digestive tract, significantly compromising individuals' health and quality of life[1,2]. According to research statistics, approximately 70% CRC are located in the left-side, including the splenic flexure, descending colon, sigmoid colon, and rectum[3]. The inferior mesenteric artery (IMA) arises from the abdominal aorta, located between the L2 and L4 vertebrae, and primarily supplies the left side of the colon and the upper portion of the rectum[4]. Usually, IMA has three branches: the left colic artery (LCA), which primarily supplies the descending colon and splenic flexure; the sigmoid arteries (SA), which primarily supply the sigmoid colon; and the superior rectal artery (SRA), which primarily supplies the upper portion of the rectum. During the surgical procedures of laparoscopic left-sided colon or rectal resection, it is crucial to meticulously handle the IMA and complete lymph node dissection (D3)[5–8]. For example, in laparoscopic anterior resection of the rectum, completing D3 lymph node dissection at the root of IMA while preserving LCA, though challenging, can reduce the incidence of postoperative complications[9,10]. For patients with tumors located in the descending colon or sigmoid colon, selectively preserving the SAR or SA during surgery can help reduce the incidence of postoperative complications[11,12]. For non-neoplastic colonic conditions, such as, inflammatory bowel disease and colonic diverticula, while lymphadenectomy is not required during surgery, careful management of the IMA branches is essential to ensure sufficient blood supply to the remaining colon and the anastomosis[13,14].

According to relevant studies, the IMA commonly exhibits four types or variations. In Type I, the LCA branches off early and separately from the IMA, followed by the SA and SRA branching together from the IMA. In Type II, the LCA and SA initially branch together from the IMA, while the SRA branches independently from the IMA. In Type III, the LCA, SA, and SRA all branch together from the IMA. In Type IV, the LCA is absent, with only the SA and SRA present[5,15]. In addition, some studies also showed that the anatomical relationships between the LCA and the IMV can be classified into four types[16–18]. In detail, medial type, the LCA ascends closely along the medial side of the IMV; overlapping type: LCA and IMV exhibit a crossing course; lateral type, the LCA ascends on the lateral side of the IMV (with a distance less than 15 mm); distant type, the LCA ascends on the lateral side of the IMV and is far away from the IMV[19]. Some studies also focus on the crossing relationship between the LCA and IMV, specifically including the type where the LCA runs across above the IMV and the type where the LCA is located dorsal to the IMV[17]. Overall, the complex anatomical classifications of the IMA/IMV and potential anatomic variation significantly increase surgical risks and present great challenges for the surgeon.

Department of Anorectal Surgery, Fuyang City People's Hospital, No. 501 Sanqing Road, Yingzhou District, Fuyang, Anhui, 236000, China. ✉e-mail: hzj130123@126.com

K. Wang[5] has previously studied the application of preserving the LCA in rectal cancer (RC) surgery through three-dimensional (3D) reconstruction. *J. Chen*[20] has investigated the impact of different IMA classifications on the preservation of the LCA using enhanced computed tomography (CT) scan. Although the aforementioned studies are excellent and have certain clinical significance, their data and figures are not open source. This limitation restricts the ability of other researchers to validate findings, conduct further analyses, and apply these insights to related studies. Open-source data promotes greater transparency, reproducibility, and collaboration across the scientific community. By making data and figures openly accessible, researchers can build upon existing work, explore new hypotheses, and accelerate the pace of discovery.3D reconstruction visualization and 3D printing technology can be utilized for medical, including medical education and training, anatomical research, personalized implants, preoperative simulation and intraoperative navigation, assisting surgeons in selecting the appropriate surgical plan[21,22]. 3D reconstruction and 3D printing technology offer significant advantages in studying the classification of the IMA. These techniques provide precise, high-resolution anatomical images, detailing the structure of the IMA and its branches, aiding in the accurate understanding of its anatomical variations and classification. Additionally, 3D printing technology can materialize the reconstructed anatomical structures, allowing researchers and clinicians to observe and manipulate physical models from different angles, enhancing the intuitive understanding of the IMA structure. In our previous retrospective studies, we found that 3D reconstruction and 3D printing of IMA models are beneficial for surgeons in preoperative simulation, allowing for the formulation of individualized treatment plans and intraoperative navigation to accurately locate key vessels. In laparoscopic rectal cancer surgery, these techniques have been shown to effectively reduce surgical risks and complexity[23]. According to this datasets research, we found that 3D-reconstructed IMA/IMV images provide a more effective platform for researchers to observe, share, and disseminate findings. This approach also offers significant advantages for advancing future research into the detailed anatomy of the IMA/IMV. As the first study to apply 3D reconstruction and 3D printing technology for exploring the anatomical classification of the IMA/IMV, this work effectively fills the existing gap of insufficient 3D datasets focusing on the IMA and IMV. Furthermore, we have made these 3D images open source to facilitate future research by other investigators. By making the data accessible, we aim to foster greater collaboration across the scientific community, accelerate advancements in anatomical research, and contribute to the improvement of clinical outcomes in colorectal surgery.

Methods

Data collection. Patients who underwent surgical treatment for rectal cancer, sigmoid colon cancer, and descending colon cancer at Fuyang City People's Hospital were included between January 2022 and May 2025. The high-resolution imaging data from RC patients undergoing abdominal surgery were collected for investigating the types of the IMA/IMV. This study utilized contrast-enhanced CT scans, which provide detailed visualization of vascular structures. In addition, the clinical characteristics (age, height, weight, gender) of patients were collected. Inclusion criteria: (1) Patients aged $\geq$ 18 years; (2) Presence of clear preoperative enhanced-CT imaging data; (3) Underwent laparoscopic surgery with intraoperative exposure of the IMA/IMV-related vessels; (4) Availability of surgical videos, images, or detailed surgical records documenting the vascular classification; (5) Provided signed informed consent. Exclusion criteria: (1) Lacking or losing clinical or imaging data; (2) History of prior surgeries that may have altered the vascular anatomy; (3) Comorbidity with schizophrenia or other mental health disorders, lack of independent behavior ability, or inability to cooperate with treatment. This study was approved by the Ethics Committee of Fuyang City People's Hospital (NO: [2024] 203). All study participants signed an informed consent form, permitting data collection for this study.

3D Reconstruction and printing. Enhanced CT scans were acquired with the following parameters: slice thickness of 0.625 mm, tube voltage of 120 kV, tube current of 250–300 mA, and contrast agent (iopromide injection) administered at a dose of 1.5 mL/kg body weight with an injection rate of 3.0–3.5 mL/s. The arterial phase images were imported in DICOM format into 3D modeling software (3D Slicer 5.2.2) for 3D reconstruction. The abdominal aorta (AA), left iliac artery, right iliac artery, IMA, LCA, SA, SRA, IMV and related artery/vein and organs were manually selected for segmentation and 3D reconstruction. And the required arteries and veins were selected and marked in the transverse, sagittal, and coronal planes in sequence. The surface of the 3D virtual model was refined through a smoothing process. After confirmation by another 3D reconstruction technician that there were no reconstruction errors, the IMA model was 3D-printed using a high-precision SLA 3D printer with white resin material. The 3D printing models were subsequently cured, polished, and color-coded, with red representing the arteries and blue representing the veins. Finally, the 3D printing models was ultimately confirmed by surgeons during the operation.

Classification of IMA and IMV Types. The intraoperative data were particularly valuable for accurately classifying the types of IMA and IMV. Surgeons assessed the IMA/IMV types and anatomical variations by enhanced CT and 3D reconstruction. The classification of IMA and IMV types was validated through real-time observations, comparison with operation videos or images, surgical records, as well as 3D reconstruction images and 3D-printed models.

IMA Classification. The IMA can be classified into four types:

Type I: The LCA branches off early and independently from the IMA, while the SA and SRA branch jointly from the IMA.

Type II: The LCA and SA branch together from the IMA, and the SRA branches independently from the IMA.

Type III: The LCA, SA, and SRA all branch jointly from the IMA.

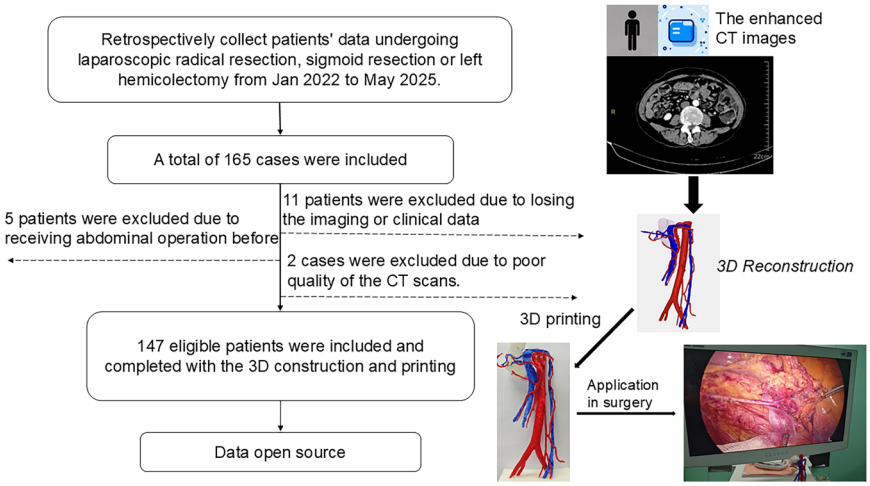


Fig. 1 The design and flowchart of this study.

Type IV: The LCA is absent, with only the SA and SRA branching from the IMA.

IMV Classification. The IMV has two kinds of classification types.

1. By spatial structural relationship among the LCA, IMA and IMV, it can be categorized into four types:
LCA medial type: LCA close medial to IMV, $D_{LCA} < D_{IMV}$;
LCA overlapping type: LCA and IMV exhibit a crossing course, $D_{LCA} = D_{IMV}$;
LCA lateral type: LCA close lateral to IMV, $D_{LCA} > D_{IMV}$ and $D_{LCA} - D_{IMV} \leq 15$ mm.;
LCA distant type: LCA distantly lateral to IMV, $D_{LCA} - D_{IMV} > 15$ mm.
2. By crossing relationship between the LCA and IMV, it can be categorized into two types:
Type A: The LCA crosses over the IMV.
Type B: The LCA passes beneath the IMV.

Observation index. Patients' basic characteristics, including gender, age, height, weight, the length of the IMA trunk, the classification of IMA/IMV were collected. We defined the length of the IMA trunk as the distance from the abdominal aorta to the first branch of IMA (origin of LCA or SRA, usually). Subsequently, we collected and conducted an analysis of additional factors. These encompassed the duration of the operation, the amount of blood loss during the operation, the quantity of lymph nodes dissected, and the incidence of lymphatic vessel and nerve invasion. Moreover, we took into account the depth of tumor invasion (T stage), the presence of lymph node metastasis (N stage), hospitalization duration, postoperative recovery duration (the time from the end of operation to discharge from the hospital) and the occurrence rate of postoperative complications such as anastomotic leakage, intestinal obstruction, and wound infection. Finally, we uploaded the relevant observational data and reconstructed 3D images as attachments for data open access.

Institutional review board statement. The study was reviewed and approved by the Institutional Review Board of Fuyang City People's Hospital (NO: [2024] 203).

Informed consent statement. All study participants provided informed written consent prior to study enrollment.

Data Records

The dataset is available at IMA/IMV 3D-reconstructed images dataset[24]. This dataset includes the gender, age, height, weight, BMI, T and N stages, as well as links to 3D reconstructed images, for a total of 147 included cases. In detail, between January 2022 and May 2025, a total of 165 patients with CRC who underwent laparoscopic radical resection, sigmoid resection or left hemicolectomy were included. Among them, 11 patients who lost the imaging data or clinical data were excluded. In addition, 5 patients who underwent abdominal operation before and were further excluded. 2 cases were excluded due to poor quality of the CT scans. Finally, a total of 147 eligible patients (63 female and 84 male) were collected and were completed with the 3D construction and printing (Fig. 1). The baseline data was shown in Table 1. Among the 147 included patients, there were 82 males and 65 females; the average age was 66.94 ± 13.07 years. According to the IMA classification, there were 73 cases of Type I, 22 cases of Type II, 44 cases of Type III, and 8 cases of Type IV. The clinical characteristics of patients with the four IMA types are presented in Table 2.

Characteristics	Cases (n = 147)
Age (years)	66.94 ± 13.07
Gender	
Female	65
Male	82
Height (cm)	163.36 ± 8.55
Weight (kg)	62.39 ± 11.17
Body mass index	23.30 ± 3.28
Location of tumor	
Descending colon	11
Sigmoid colon	53
Rectum	83
AJCC stage	
I-II	105
III	42
T stage	
T1-T2	52
T3-T4	95
N stage	
N0	105
N+	42
Lymph vessel invasion	
Yes	43
No	104
Nerve invasion	
Yes	22
No	125
Postoperative complications	
Anastomotic leakage	7
Intestinal obstruction	2
Wound infection	5
Surgical duration (min)	200.71 ± 42.43
Intraoperative blood loss (ml)	44.32 ± 37.47
Postoperative recovery duration (day)	11.86 ± 8.58
Hospitalization duration (day)	18.35 ± 10.46
The length of the IMA trunk (mm)	39.55 ± 8.16
Classification of IMA	
I	73 (49.66%)
II	22 (14.97%)
III	44 (29.93%)
IV	8 (5.44%)
Classification of IMV (n = 139)	
A	111 (79.86%)
B	28 (20.14%)
Lateral type	35 (25.18%)
Medial type	47 (33.81%)
Crossing type	41 (29.50%)
Distant type	16 (11.51%)

Table 1. The baseline data of patients.

Technical Validation

To assess the quality of the image dataset, we compared the 3D reconstruction models and 3D-printed models with intraoperative operation images, as well as preoperative and postoperative contrast-enhanced CT images. As shown in Fig. 2, the 3D reconstructed images and 3D-printed models are highly consistent with the actual intraoperative anatomy, which indicates that both the 3D images and 3D-printed models have a high degree of reliability.

Typing result of IMA and IMV. Based on the classification of the IMA and the spatial structural relationship among the LCA, IMA, and IMV, we conducted relevant statistics and presented the results. As shown in

Characteristics	I	II	III	IV	F/χ2	P-value
Gender					4.867	0.182
Male	47	9	22	4		
Female	26	13	22	4		
Age (year)	66.63 ± 12.89	69.82 ± 11.00	64.68 ± 13.76	76.75 ± 9.34	2.384	0.072
Height (cm)	164.99 ± 9.11	159.68 ± 8.22	163.20 ± 7.11	159.50 ± 6.76	2.875	**0.038**
Weight (kg)	63.42 ± 12.06	61.36 ± 11.73	61.72 ± 9.41	59.63 ± 8.93	0.476	0.700
BMI (kg/m^2)	23.19 ± 3.37	23.86 ± 3.02	23.15 ± 3.09	23.54 ± 3.88	0.284	0.837
IMV Classification						
Spatial structural relationship among the LCA, IMA and IMV					4.979	0.547
Medial type	18	8	9	/		
Crossing type	24	6	11	/		
Lateral type	25	6	16	/		
Distant type	6	2	8	/		
Crossing relationship between the LCA and IMV					2.701	0.259
Type A	55	20	36	/		
Type B	18	2	8	/		
The length of the IMA trunk (mm)	37.43 ± 8.83	41.98 ± 5.73	40.42 ± 6.03	47.41 ± 10.00	5.072	**0.002**
Surgical duration (min)	196.99 ± 48.06	195.91 ± 26.31	207.61 ± 36.85	210.00 ± 45.75	0.788	0.502
Intraoperative blood loss (ml)	46.78 ± 42.82	45.91 ± 26.74	39.55 ± 33.91	43.75 ± 24.46	0.349	0.789
Postoperative recovery duration (day)	12.21 ± 9.70	10.64 ± 6.53	11.14 ± 6.85	16.00 ± 9.38	0.905	0.440
Hospitalization duration (day)	18.79 ± 11.12	16.04 ± 7.21	18.39 ± 10.74	20.50 ± 9.12	0.504	0.680
T					0.854	0.837
T1/T2	26	6	17	3		
T3/T4	47	16	27	5		
N					1.709	0.635
N0	50	17	31	7		
N+	23	5	13	1		
Lymph vessel invasion					1.673	0.643
Yes	24	6	12	1		
No	49	16	32	7		
Nerve invasion					0.340	0.952
Yes	10	4	7	1		
No	63	18	37	7		

Table 2. Clinical characteristics and comparative analysis of the four inferior mesenteric artery types. BMI: body mass index; IMA: inferior mesenteric artery; IMV: inferior mesenteric vein; LCA: left colic artery.

Fig. 3, statistical data reveal that there were 73 cases of Type I in total (the LCA branches independently from the IMA, while the SA and SRA branch jointly from the IMA), accounting for 49.66%.

Furthermore, among these cases, the subtypes were distributed as follows:

Lateral type (LCA located close to the lateral side of IMV): 18 cases, accounting for 12.24% (Fig. 3A);

Crossing type (LCA and IMV showing a crossing course): 24 cases, accounting for 16.32% (Fig. 3B);

Medial type (LCA located close to the medial side of IMV): 25 cases, accounting for 17.01% (Fig. 3C);

Distant type (LCA located distantly on the lateral side of IMV, with a distance >15 mm): 6 cases, accounting for 4.08% (Fig. 3D).

In addition, as shown in Fig. 4, there were 22 cases of Type II in total (the LCA and SA branch together from the IMA, and the SRA branches independently from the IMA), accounting for 14.97%. And the subtypes were distributed as follows:

Lateral type: 8 cases, accounting for 5.44% (Fig. 4A);

Crossing type: 6 cases, accounting for 4.08% (Fig. 4B);

Medial type: 6 cases, accounting for 4.08% (Fig. 4C);

Distant type: 2 cases, accounting for 1.36% (Fig. 4D).

In addition, as shown in Fig. 5, there were 44 cases of Type III in total (The LCA, SA, and SRA all branch jointly from the IMA), accounting for 29.93%. And the subtypes were distributed as follows:

Lateral type: 9 cases, accounting for 6.12% (Fig. 5A);

Crossing type: 11 cases, accounting for 7.48% (Fig. 5B);

Medial type: 16 cases, accounting for 10.88% (Fig. 5C);

Distant type: 8 cases, accounting for 5.44% (Fig. 5D).

Besides, there were 8 cases of Type IV in total (The LCA is absent, with only the SA and SRA branching from the IMA), accounting for 5.44% (Fig. 6). Based on the crossing relationship between the LCA and IMV, our statistical analysis showed the following: there were 111 cases where the LCA crossed over the IMV, accounting

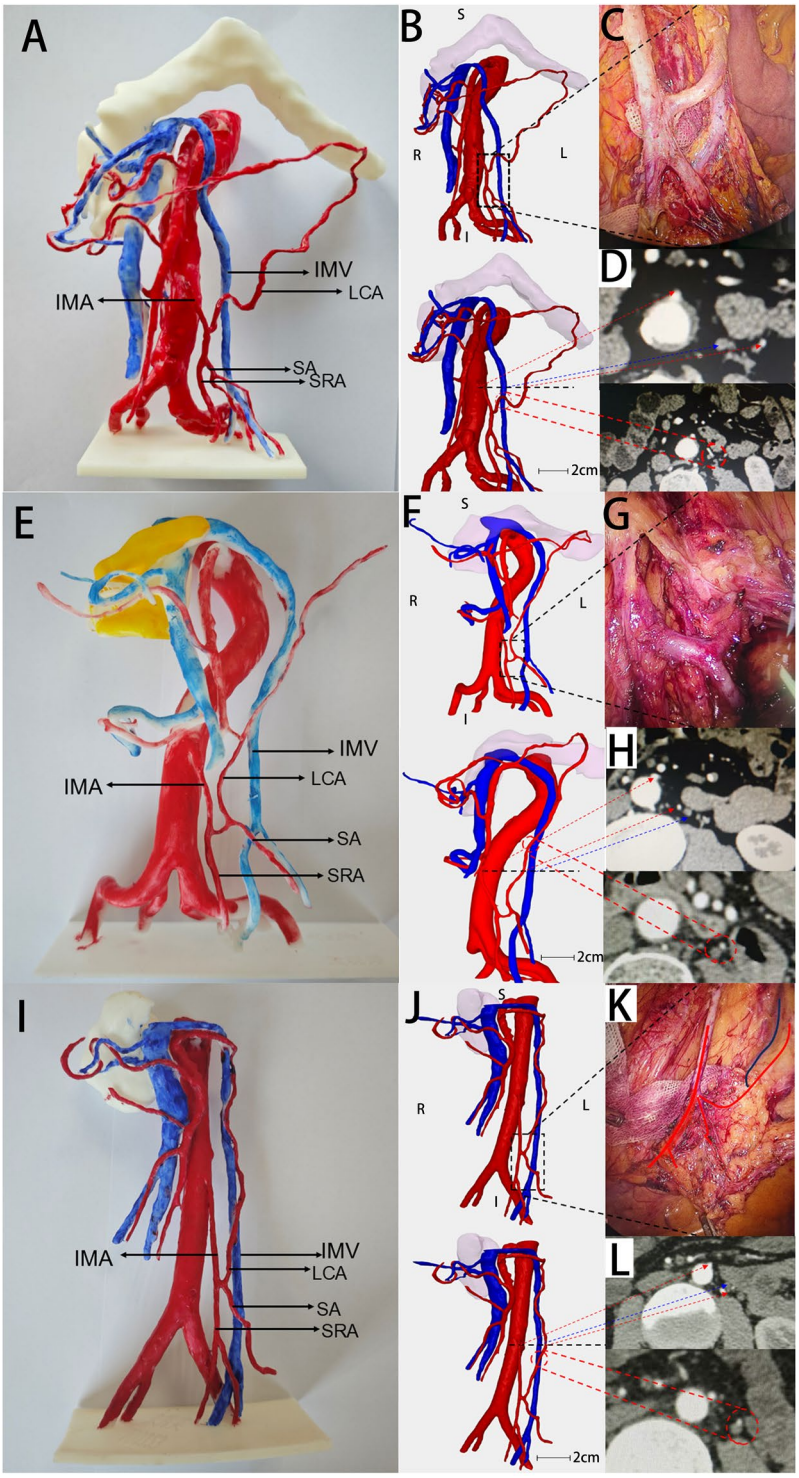


Fig. 2 Comparison of three-dimensional (3D) printed models and 3D reconstructed images of the inferior mesenteric artery and vein (IMA/IMV) and their surrounding organs with enhanced computed tomography (CT) images and intraoperative photographs, demonstrating the excellent accuracy of 3D reconstruction images and 3D-printed models. (**A**) 3D-printed model of IMA Type I; (**B**) 3D reconstructed image of IMA Type I; (**C**) Intraoperative real anatomical photograph of IMA Type I; (**D**) Enhanced CT image of IMA Type I (Axial). (**E**) 3D-printed model of IMA Type II; (**F**) 3D reconstructed image of IMA Type II; (**G**) Intraoperative real anatomical photograph of IMA Type II; (H) Enhanced CT image of IMA Type II (Axial). (**I**) 3D-printed model of IMA Type III; (**J**) 3D reconstructed image of IMA Type III; (**K**) Intraoperative real anatomical photograph of IMA Type III; (**L**) Enhanced CT image of IMA Type III (Axial). Red represents arteries, and blue represents veins.

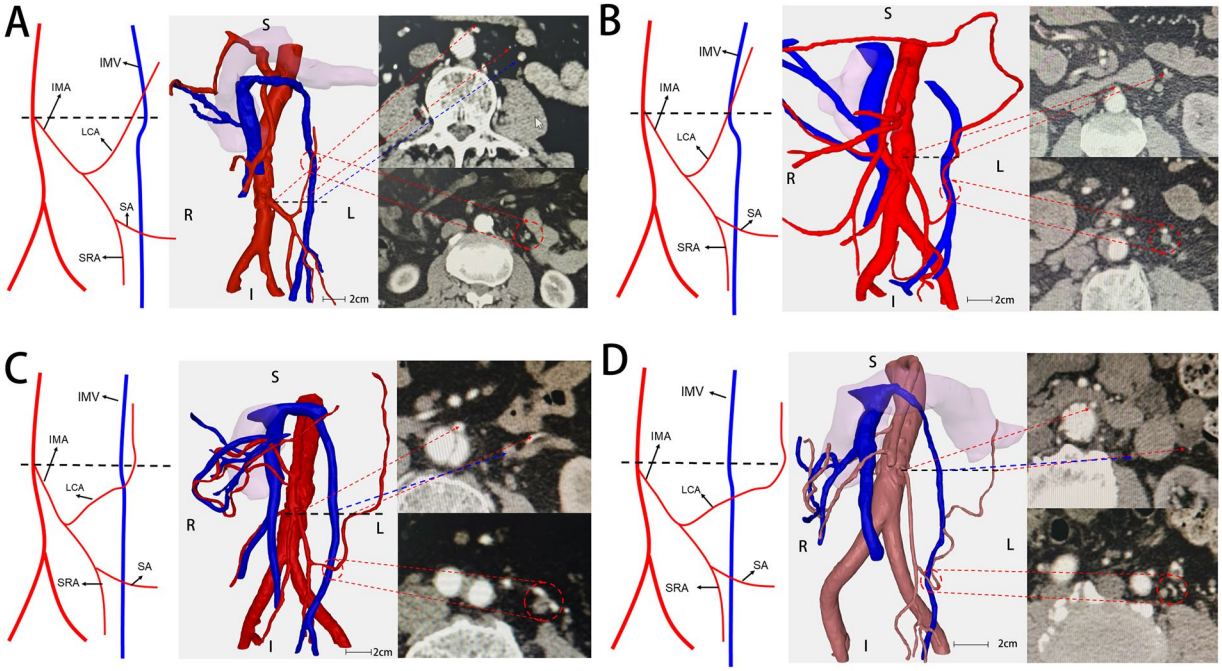


Fig. 3 Schematic diagram (left), 3D reconstructed image (middle), and enhanced CT image (right) of IMA Type I (the left colic artery (LCA) arising solely from the main trunk of the IMA, (49.66%)). (**A**) Lateral type (12.24%): LCA located close to the lateral side of the IMV. (**B**) Crossing type (16.32%): LCA and IMV showing a crossing course. (**C**) Medial type (17.01%): LCA located close to the medial side of IMV (distance $\leq$ 15 mm). (**D**) Distant type (4.08%): LCA located distantly on the lateral side of IMV (distance $>$ 15 mm). The enhanced CT images are in the axial plane. Red represents arteries, and blue represents veins.

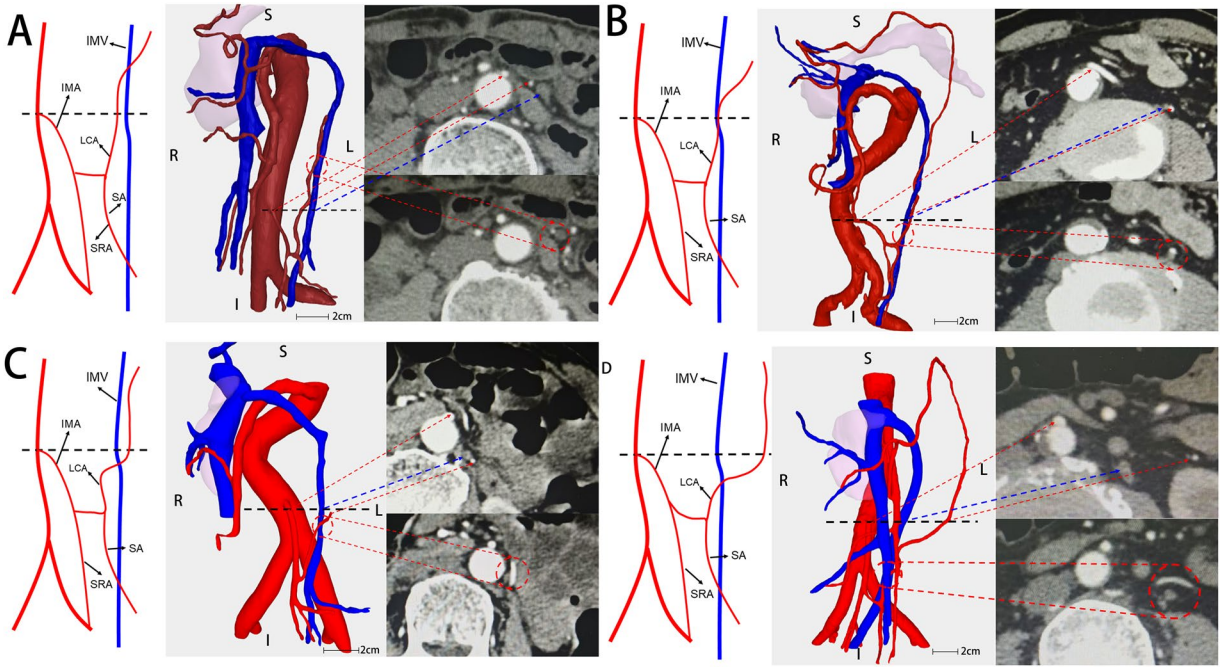


Fig. 4 Schematic diagram (left), 3D reconstructed image (middle), and enhanced CT image (right) of IMA Type II (LCA and sigmoid artery (SA) branching conjointly from the main trunk of the IMA, with the superior rectal artery (SRA) branching independently from the IMA). (**A**) Lateral type (5.44%): LCA located close to the lateral side of the IMV. (**B**) Crossing type (4.08%): LCA and IMV showing a crossing course. (**C**) Medial type (4.08%): LCA located close to the medial side of the IMV (distance $\leq$ 15 mm). (**D**) Distant type (1.36%): LCA located distantly on the lateral side of the IMV (distance $>$ 15 mm). The enhanced CT images are in the axial plane. Red represents arteries, and blue represents veins.

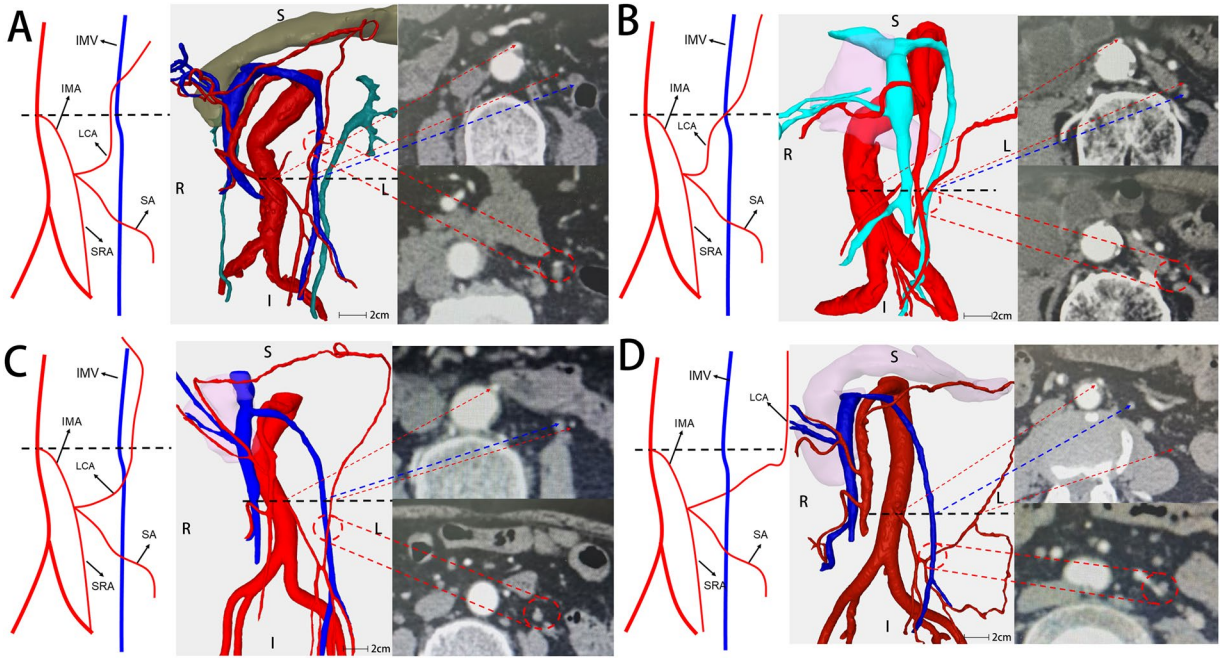


Fig. 5 Schematic diagram (left), 3D reconstructed image (middle), and enhanced CT image (right) of IMA Type III (LCA, SA, and SRA all branch jointly from the IMA). (**A**) Lateral type (6.12%): LCA located close to the lateral side of the IMV. (**B**) Crossing type (7.48%): LCA and IMV showing a crossing course. (**C**) Medial type (10.88%): LCA located close to the medial side of the IMV (distance $\leq$ 15 mm). (**D**) Distant type (5.44%): LCA located distantly on the lateral side of the IMV (distance $>$ 15 mm). The enhanced CT images are in the axial plane. Red represents arteries, and blue represents veins.

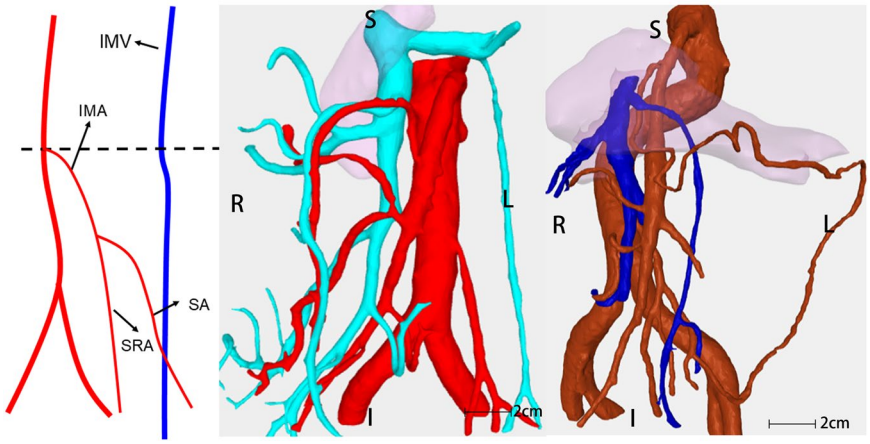


Fig. 6 Diagram and 3D reconstruction image display of IMA Type IV, in which the LCA is absent and only the SA and SRA branch from the IMA, accounting for 5.44%. Red represents arteries, and blue represents veins.

for 79.86% (Figs. 3–5); and 28 cases where the LCA passed beneath the IMV, accounting for 20.14% (Fig. 7A,B). In total, our dataset is consistent with previous related high-quality research data[15–17,19]. Furthermore, this dataset is the first to present the anatomical morphology of the IMA and IMV in the form of 3D visualization, with the complex spatial anatomical relationships between the IMA and IMV also successfully demonstrated in detail. For the limitations, we honestly acknowledge the following points. First, this is a single-center retrospective study, and the sample is derived from CRC patients, which may limit the generalizability of the dataset to healthy populations or patients with other digestive system diseases. Second, the dataset does not include long-term follow-up data of patients, so it cannot reflect the correlation between IMA/IMV anatomical types and long-term surgical outcomes. Finally, due to technical constraints, the dataset does not provide quantitative parameters such as vascular wall thickness and blood flow velocity, which may restrict certain in-depth biomechanical research.

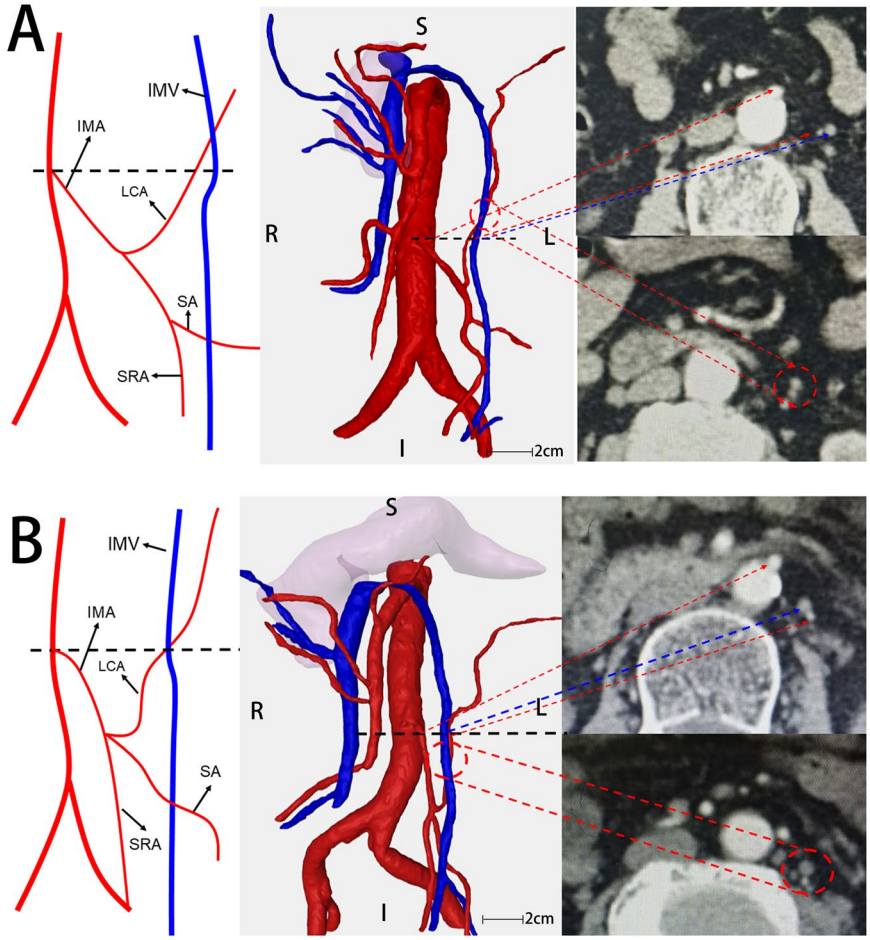


Fig. 7 Schematic diagram (left), 3D reconstructed image (middle), and enhanced CT image (right), showing the LCA running beneath the IMV, with this type accounting for 20.14%. The enhanced CT images are in the axial plane. Red represents arteries, and blue represents veins.

Data availability

The dataset included in this study can be obtained from *Figshare* https://doi.org/10.6084/m9.figshare.30529484. All research data included in this study was obtained with the explicit consent of participants, who have expressly agreed to the public sharing of such data.

Code availability

No custom code was generated or used in the present study.

Received: 15 September 2025; Accepted: 15 December 2025;
Published online: 24 December 2025

References

1. Siegel, R. L., Giaquinto, A. N. & Jemal, A. Cancer statistics, 2024. *CA Cancer J Clin* **74**, 12–49, https://doi.org/10.3322/caac.21820 (2024).
2. Siegel, R. L., Miller, K. D., Wagle, N. S. & Jemal, A. Cancer statistics, 2023. *CA Cancer J Clin* **73**, 17–48, https://doi.org/10.3322/caac.21763 (2023).
3. Krul, M. F. *et al.* Initial Impact of National CRC Screening on Incidence and Advanced Colorectal Cancer. *Clin Gastroenterol Hepatol* **21**, 797–807 e793, https://doi.org/10.1016/j.cgh.2022.08.046 (2023).
4. Balcerzak, A., Kwasniewska, O., Podgorski, M., Olewnik, L. & Polguj, M. Types of inferior mesenteric artery: a proposal for a new classification. *Folia Morphol (Warsz)* **80**, 827–838, https://doi.org/10.5603/FM.a2020.0115 (2021).
5. Wang, K. X., Cheng, Z. Q., Liu, Z., Wang, X. Y. & Bi, D. S. Vascular anatomy of inferior mesenteric artery in laparoscopic radical resection with the preservation of left colic artery for rectal cancer. *World J Gastroenterol* **24**, 3671–3676, https://doi.org/10.3748/wjg.v24.i32.3671 (2018).
6. Li, Z., Zhou, Y., Xu, L. & Xie, L. Safety and efficacy of left colic artery preservation in laparoscopic anterior resection for lower rectal cancer. *Future Oncol* **19**, 1485–1494, https://doi.org/10.2217/fon-2023-0475 (2023).
7. Lange, M. M., Buunen, M., van de Velde, C. J. & Lange, J. F. Level of arterial ligation in rectal cancer surgery: low tie preferred over high tie. A review. *Dis Colon Rectum* **51**, 1139–1145, https://doi.org/10.1007/s10350-008-9328-y (2008).
8. Patroni, A. *et al.* Technical difficulties of left colic artery preservation during left colectomy for colon cancer. *Surg Radiol Anat* **38**, 477–484, https://doi.org/10.1007/s00276-015-1583-8 (2016).

9. Liu, F. C., Song, J. N., Yang, Y. C. & Zhang, Z. T. Preservation of left colic artery in laparoscopic colorectal operation: The benefit challenge. *World J Gastrointest Surg* **15**, 825–833, https://doi.org/10.4240/wjgs.v15.i5.825 (2023).
10. Zhang, C. *et al*. The feasibility of laparoscopic TSME preserving the left colic artery and superior rectal artery for upper rectal cancer. *World J Surg Oncol* **18**, 212, https://doi.org/10.1186/s12957-020-01986-6 (2020).
11. Tang, X. *et al*. Preservation of the left colic artery and superior rectal artery in laparoscopic surgery can reduce anastomotic leakage in sigmoid colon cancer. *J Minim Access Surg* **17**, 208–212, https://doi.org/10.4103/jmas.JMAS_15_20 (2021).
12. Borchert, D. H. *et al*. Observational study on preservation of the superior rectal artery in sigmoid resection for diverticular disease. *Int J Surg* **21**, 45–50, https://doi.org/10.1016/j.ijsu.2015.07.011 (2015).
13. Dunleavy, K. A. *et al*. Total Proctocolectomy vs Subtotal/total Colectomy for Neoplasia in Patients With Inflammatory Bowel Disease and Primary Sclerosing Cholangitis. *Inflamm Bowel Dis*, https://doi.org/10.1093/ibd/izad278 (2023).
14. Hennessy, O., Egan, L. & Joyce, M. Subtotal colectomy in ulcerative colitis-long term considerations for the rectal stump. *World J Gastrointest Surg* **13**, 198–209, https://doi.org/10.4240/wjgs.v13.i2.198 (2021).
15. Ding, Y. *et al*. Assessing anatomical variations of the inferior mesenteric artery via three-dimensional CT angiography and laparoscopic colorectal surgery: a retrospective observational study. *Sci Rep* **14**, 6985, https://doi.org/10.1038/s41598-024-57661-3 (2024).
16. Zhang, H. *et al*. The Atlas of the Inferior Mesenteric Artery and Vein under Maximum-Intensity Projection and Three-Dimensional Reconstruction View. *J Clin Med* **13**, https://doi.org/10.3390/jcm13030879 (2024).
17. Murono, K. *et al*. Anatomy of the inferior mesenteric artery evaluated using 3-dimensional CT angiography. *Dis Colon Rectum* **58**, 214–219, https://doi.org/10.1097/DCR.0000000000000285 (2015).
18. Zhou, J. *et al*. A study on spinal level, length, and branch type of the inferior mesenteric artery and the position relationship between the inferior mesenteric artery, left colic artery, and inferior mesenteric vein. *BMC Med Imaging* **22**, 38, https://doi.org/10.1186/s12880-022-00764-y (2022).
19. Ke, J. *et al*. Anatomic variations of inferior mesenteric artery and left colic artery evaluated by 3-dimensional CT angiography: Insights into rectal cancer surgery - A retrospective observational study. *Int J Surg* **41**, 106–111, https://doi.org/10.1016/j.ijsu.2017.03.012 (2017).
20. Chen, J. *et al*. A clinical study of inferior mesenteric artery typing in laparoscopic radical resections with left colonic artery preservation of rectal cancer. *World J Surg Oncol* **20**, 292, https://doi.org/10.1186/s12957-022-02762-4 (2022).
21. Khorsandi, D. *et al*. 3D and 4D printing in dentistry and maxillofacial surgery: Printing techniques, materials, and applications. *Acta Biomater* **122**, 26–49, https://doi.org/10.1016/j.actbio.2020.12.044 (2021).
22. Zoabi, A. *et al*. 3D Printing and Virtual Surgical Planning in Oral and Maxillofacial Surgery. *J Clin Med* **11**, https://doi.org/10.3390/jcm11092385 (2022).
23. Zhao, Z. X. *et al*. Three-dimensional printing for preoperative rehearsal and intraoperative navigation during laparoscopic rectal cancer surgery with left colic artery preservation. *World J Gastrointest Surg* **16**, 3104–3113, https://doi.org/10.4240/wjgs.v16.i10.3104 (2024).
24. Zhao, Z. A single-center 3D reconstruction image dataset for exploring inferior mesenteric artery and vein types. *figshare. Dataset.* https://doi.org/10.6084/m9.figshare.30529484.v1 (2025).

Acknowledgements

This study was supported by the Health Commission of Fuyang City, Anhui Provence, China (NO. FY2021-18 and NO. FY2023-45) and the Health Commission Anhui Provence, China (NO. AHWJ2023BAa20164) and Bureau of Science and Technology of Fuyang City, Anhui Provence, China (NO.FK20245505).

Author contributions

Zhao Z.X. and Yao Y. designed the study and wrote the manuscript; Hu Z.J. instructed the whole study and prepared the figures; Su X.Y. and Zhu S. collected and analyzed the data; Hu Z.J. performed the operations; all authors have approved the final version of the manuscript.

Competing interests

The authors declare no competing interests.

Additional information

Correspondence and requests for materials should be addressed to Z.H.

Reprints and permissions information is available at www.nature.com/reprints.

Publisher's note Springer Nature remains neutral with regard to jurisdictional claims in published maps and institutional affiliations.

Open Access This article is licensed under a Creative Commons Attribution-NonCommercial-NoDerivatives 4.0 International License, which permits any non-commercial use, sharing, distribution and reproduction in any medium or format, as long as you give appropriate credit to the original author(s) and the source, provide a link to the Creative Commons licence, and indicate if you modified the licensed material. You do not have permission under this licence to share adapted material derived from this article or parts of it. The images or other third party material in this article are included in the article's Creative Commons licence, unless indicated otherwise in a credit line to the material. If material is not included in the article's Creative Commons licence and your intended use is not permitted by statutory regulation or exceeds the permitted use, you will need to obtain permission directly from the copyright holder. To view a copy of this licence, visit http://creativecommons.org/licenses/by-nc-nd/4.0/.

© The Author(s) 2025